RESEARCH ARTICLE



Continuous oil/water separation using LDH-based membranes with inverse wettability

Maryam Davardoostmanesh¹ · Negin Gorgani¹ · Hossein Ahmadzadeh¹

Received: 21 November 2024 / Accepted: 7 July 2025 © The Author(s), under exclusive licence to Springer-Verlag GmbH Germany, part of Springer Nature 2025

Abstract

Oil spills and industrial oily wastewater pollution are two global environmental problems that necessitate the separation of oil and water. In this work, we present a novel continuous separation system based on two membranes with inverse wettability, both derived from a single adsorbent layered double hydroxide (LDH) through minimal surface modification. Drawing inspiration from biological surfaces, a superhydrophilic/underwater superoleophobic membrane was prepared by coating micro/nanostructured stainless-steel mesh with LDH, mimicking the wetting behavior of fish scales. A simple post-modification with stearic acid transformed the same LDH coating into a superhydrophobic/superoleophilic membrane, inspired by lotus leaf surfaces. These two complementary membranes were integrated into a bidirectional system capable of continuous and efficient separation of both light and heavy oil/water mixtures. The system achieved separation efficiencies over 98% and an ultrahigh flux of 105,000 Lm⁻²h⁻¹. This study demonstrates a cost-effective, scalable approach to continuous oil/water separation using a single functional material, significantly advancing membrane design for environmental remediation.

Keywords LDH · Wettability · Fish scales · Lotus leaf · Oil/water mixture · Continuous separation

Introduction

Water pollution arising from oil spill accidents and industrial oily wastewater has led to the discharge of large amounts of effluents into the environment and has created difficulties in initial treatment (Davardoostmanesh and Ahmadzadeh 2021; Chen et al. 2022). In recent years, membrane separation and filtration technology has attracted tremendous attention in the field of oil/water separation due to high efficiency, simplicity, and energy saving (Singh et al. 2022, 2025a; Xin et al. 2024). In this regard, various superwetting membranes have been developed based on the different wettability values of oil and water (Li et al. 2022). These superwetting membranes are constructed by introduction of hierarchical rough structure on the special surfaces and classified into two categories including superhydrophobic/superoleophilic and superhydrophilic/underwater superoleophobic membranes

Responsible Editor: Angeles Blanco

Published online: 17 July 2025

(Sow et al. 2021; Davardoostmanesh and Ahmadzadeh 2023b, a).

A superhydrophobic/superoleophilic surface strongly repels water, causing water droplets to bead and roll off due to a contact angle greater than 150°, while simultaneously attracting and absorbing oil with a near-zero oil contact angle (Singh et al. 2025b). In contrast, a superhydrophilic/underwater superoleophobic surface exhibits extreme water affinity and oil repellency when submerged in water. Specifically, such surfaces allow water to spread completely with a contact angle less than 10°, while repelling oil underwater with an oil contact angle greater than 150°. This dual behavior makes them highly effective for oil—water separation, as water passes through while oil is blocked.

A typical example of superhydrophobic surface in nature is lotus leaf (Wang 2023). The surface of the lotus leaf cannot be wetted by water because of inherent hydrophobicity (Xu et al. 2021). A water droplet rolls away from the surface of lotus leaf and take away the adherent pollutants which is called "lotus effect" (Han et al. 2024). The surface of lotus leaf is covered by a micro-sized rough layer which is covered by a nano-sized waxy layer of hydrophobic crystalloids (Zhao et al. 2022). Inspired by lotus leaf, the superhydrophobic and superoleophilic membranes have



Department of Chemistry, Faculty of Science, Ferdowsi University of Mashhad, Mashhad 9177948974, Iran

been developed for separation of heavy oil/water mixture $(\rho_{oil} > \rho_{water})$ (Qing et al. 2020). Because, the water layer settled on the membrane surface prevents light oil permeation. On the contrary, fish can resist oil pollution in water in a way similar to the lotus effect in the atmosphere possessing an antifouling mechanism. The hydrophilic nature of fish scales is due to a thin layer of mucus on its surface (Jiang and Lin 2015). It has been reported that the hydrophilic surface of fish scales shows superoleophobicity after being immersed in water (Jiang and Lin 2015; Liu et al. 2021). Thus, the superhydrophilic and underwater superoleophobic membranes have been created inspired by fish scale (Zhou et al. 2021; Liu et al. 2021). These types of membranes are more suitable for the separation of light oil/ water mixtures ($\rho_{oil} < \rho_{water}$) because the barrier layer created by the heavy oil prevents water from passing through the membrane (Dai et al. 2020). Thus, each one of membranes is more appropriated for separation of a different type of oil/water mixture (light or heavy oil/water mixture) (Kang et al. 2018). On the other hands, owing to the maximum intrusion pressure created by the accumulated phase, these membranes are only employed for batch separation process, which limits scalable applications (Li et al. 2018, 2022). With the purpose of continuous separation, integration of two types of membranes with inverse wettability in a single separation device can be a breakthrough (Gong et al. 2020).

Therefore, this work aims to use a continuous separation system using a pair of superwetting membranes with inverse wettability based on the same coating for oil/water separation regardless of oil density. This continuous oil/water separation system contains two types of membranes: one with high surface energy (fish-scale effect) and another with low surface energy (lotus effect).

Layered double hydroxides (LDHs) are type of synthetic anionic clay consist of exchangeable anions between positively charged brucite-like hydroxide layers (George et al. 2024). Recently, LDH compounds have been developed for modification of metallic mesh substrates for oil/water separations (Liu et al. 2019; Xie et al. 2020; Xiang et al. 2021). Xiang et al.(2021) prepared superhydrophobic surface by coating FeNi-LDH on the surface of steel mesh followed by further modification with triethoxy(octyl) silane to decrease the surface energy. LDH can achieve strong electrostatic interaction on the surface of steel mesh through hydroxyl groups on its structure (Xie et al. 2020).

In this work, a versatile membrane platform was prepared by depositing LDH onto a stainless-steel mesh via a simple hydrothermal method. The intrinsic hydrophilicity of LDH, combined with the micro/nano-roughness induced on the mesh surface, endowed the membrane with superhydrophilic and underwater superoleophobic properties. Remarkably, this same LDH-based surface

was transformed into a superhydrophobic/superoleophilic membrane through a straightforward post-treatment with stearic acid (SA), eliminating the need for additional materials or complex fabrication steps. Leveraging this material-efficient strategy, a bidirectional separation device was assembled by integrating the two LDH-derived membranes with opposing wettabilities. This system enabled the continuous and high-flux separation of both light and heavy oil/water mixtures, highlighting a scalable, dual-function approach for advanced environmental remediation.

SA was selected as the hydrophobic modification agent due to several favorable characteristics that align with the design goals of the separation system. Firstly, SA is a long-chain fatty acid with a hydrophobic tail that effectively lowers surface energy when grafted onto a substrate, thereby enhancing water repellency. This makes SA ideal for converting hydrophilic surfaces, such as LDH-coated meshes, into superhydrophobic ones. Secondly, SA is widely used in surface modification applications because it readily forms a stable monolayer through chemical or physical interactions with hydroxyl-rich surfaces such as LDH. This compatibility ensures a uniform coating and long-term stability of the modified mesh. Moreover, SA is a low-cost, environmentally benign material, which supports the overall goal of developing a scalable and sustainable oil/water separation system.

The steel mesh modified with only SA exhibits superhydrophobic and oleophilic behavior but lacks the hierarchical micro/nanostructure provided by the LDH coating, which is crucial for achieving high separation efficiency and flux. Compared to the membrane modified with SA and LDH, the SA-modified membrane shows inferior oil permeability and mechanical stability under continuous operation, confirming the synergistic role of the LDH layer and SA in optimizing surface roughness and wettability. This comparison highlights the necessity of LDH in achieving the high-performance separation observed in our dual-membrane system.

Previous studies have frequently exploited LDH-coated meshes for batch or gravity-driven oil/water separation, but these systems operate in a single direction and cannot sustain a continuous process. For example, Xie et al. (2020) reported an MgAlZn-LDH mesh that achieved high efficiency yet functioned only in static mode. In contrast, our work uses one adsorbent, LDH, and only a mild post-treatment with stearic-acid to create membranes with two opposite wettability that are integrated into a single bidirectional device. This LDH-only platform simultaneously handles light and heavy oils under continuous flow, delivering ultrahigh fluxes while eliminating the material mismatches and staging losses that limit earlier LDH membranes. To the best of our knowledge, this is the first demonstration of an LDH-based system that provides continuous, dual-direction oil/water separation



within one compact module, marking a substantive advance over conventional, one-shot LDH separators.

Experimental

Material and methods

Material Stainless steel mesh (SSM, mesh 300) was supplied by a local store. Hydrofluoric acid (HF, 40%), Al(NO₃)₃·9H₂O (99%), stearic acid (SA, > 98%), and urea (> 95%) were provided by Merck. Zn(NO₃)₂·6H₂O (99%) and Mg(NO₃)₂·6H₂O (98%) were purchased from Riedel. All of organic solvents were supplied from Mojallali (Iran).

Instrument The FE-SEM images of the pure and coated meshes were recorded by TESCAN-XMU instrument. A Thermo Nicolet Avatar 370 FT-IR Spectrometer was used to record FT-IR spectra of the samples in the range 500 to $4000~\rm cm^{-1}$. A commercial contact angle (CA) system of 5 V-USB port power source was used to measure oil contact angle (OCA) and water contact angle (WCA) by injecting 3 μ L oil or water droplets onto the mesh surface.

Preparation of superwetting membranes

The SSMs with size of 3×3 cm² were used as substrate. Prior to coating, the SSM pieces were dipped in the HF solution to be oxidized for 10 min. Then, the activated meshes were transferred into an autoclave containing a mixed solution of Al(NO₃)₃·9H₂O (0.100 mol L⁻¹), Mg(NO₃)₂·6H₂O (0.096 mol L⁻¹), Zn(NO₃)₂·6H₂O (0.100 mol L⁻¹), and urea (2.092 mol L⁻¹) at 90 °C for 12 h. The superhydrophilic mesh was obtained after cleaning with deionized water (SSM-LDH). The prepared SSM-LDH was immersed into SA-ethanol solution at 25 °C for 12 h. The superhydrophobic mesh was obtained after rinsing with ethanol and drying at 50 °C (SSM-LDH/SA).

Oil-water separation

For oil/water separation, the desired mesh was sandwiched between two plastic tubes. Two different types of functionalized meshes were used based on the oil density. The superhydrophilic mesh (SSM-LDH) was used for light oil/water separation and the superhydrophobic mesh (SSM-LDH/SA) was used for heavy oil/water separation. The superhydrophilic mesh was pre-wetted by distilled water before each separation, which is essential for maintaining underwater superoleophobicity. The separation was conducted by

passing the oil/water mixture with driving force of gravity through each type of meshes.

A T-shaped bidirectional tube was designed to continuously separate all kinds of oil/water mixtures regardless of density relationship. Each type of superwetting meshes was located on one side of the T-shaped tube. The superhydrophobic side allows oil and the superoleophobic side allows water to pass through.

The oil/water separation efficiency ($\%\eta$) was calculated according to following equations, respectively (Davardoostmanesh and Ahmadzadeh 2023a):

$$\%\eta = \frac{M}{M_0} \times 100\tag{1}$$

where M_0 and M are the weights of the initial and collected oil or water, respectively. The permeation flux $(F,Lm^{-2}h^{-1})$ was calculated using the following equation (Foroutan et al. 2025):

$$F = \frac{V}{ST} \tag{2}$$

where V is the volume of permeated water (L), S is the effective contact area of the membrane (m²), and T is the separation time (h).

Permeation flux was evaluated by passing 20 mL of oil or water through each membrane. The intrusion pressure *P* (Pa) was defined as follows (Zhang et al. 2020a):

$$P = \rho g h_{max} \tag{3}$$

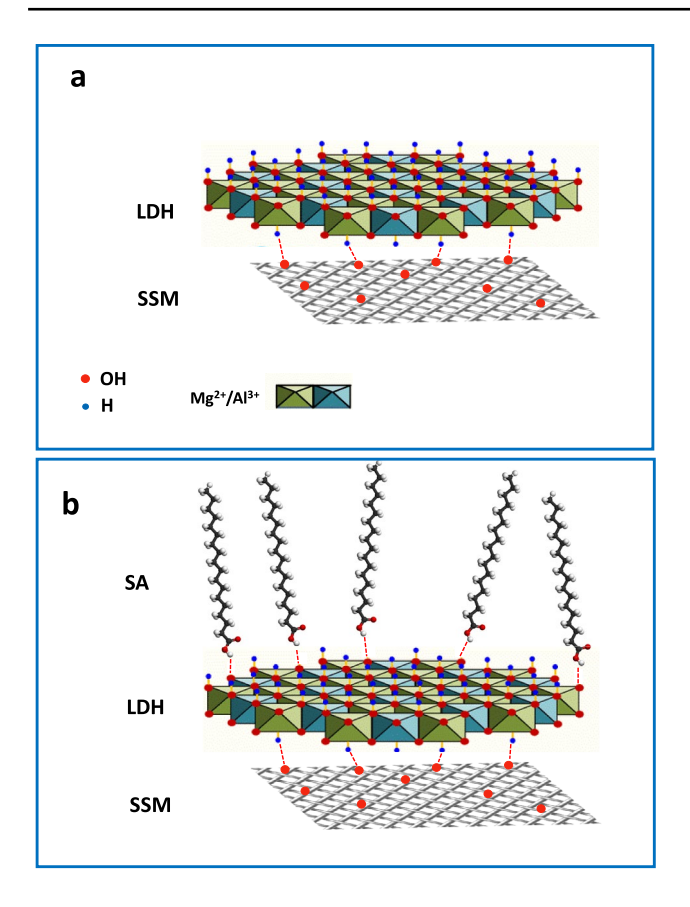
where g is the gravity (9.80 m/s²), ρ and h_{max} are the density (kg/m³) and the maximum height (m) of intercepted phase, respectively.

Results and discussions

Membrane preparation

The overall preparation process of SSM-LDH and SSM-LDH/SA is illustrated in Scheme 1. A piece of SSM was first etched by the HF solution to roughen the surface, then LDH film was grown on SSM surface under hydrothermal treatment. During the hydrothermal process, LDHs firmly bond onto the rough SSM surface via hydrogen bonds creating superhydrophilic/underwater superoleophobic surface (Xie et al. 2020). Then, the LDH coated mesh was immersed into SA solution producing superhydrophobic/superoleophilic surface based on strong hydrogen bonds interaction between hydroxyl groups in LDH and carboxylic functional groups in SA (Liu et al. 2019). SA contains a long aliphatic chain enhancing hydrophobic properties of the mesh.





Scheme 1 The preparation process of (a) superhydrophilic SSM-LDH and (b) superhydrophobic SSM-LDH/SA

Surface characterization

It is confirmed that the desired wettability of surfaces can be achieved by controlling the surface morphology through creating of hierarchical micro/nano-structure and by surface energy through tuning of the surface chemical composition. The surface morphology was investigated by FE-SEM imaging. The FE-SEM images of the pure mesh, SSM-LDH, and SSM-LDH/SA at different magnifications are shown in Fig. 1a-c. Figure 1a1-a3 shows the smooth surface of the pure mesh with an average pore diameter of about 50 μ m. After hydrothermal synthesis, flower-like spherical hierarchical structures were formed due to the in-situ growth of LDH on the mesh surface (Fig. 1b1-b3). Higher magnification FE-SEM images show clear nanoscale roughness similar to fan-shaped fish scales which might play an important role in the superoleophobicity (Fig. 1b3). Figure 1c1-c3 shows SSM-LDH/SA surface containing micro/nanoscale structures, which are similar to the lotus leaf surface. As can be seen from high magnified Fig. 1c3, these hierarchical structures are composed of many nanosheets clustered together in flower-like appearance. These morphologies greatly enhance the surface roughness, which is essential for superhydrophobicity of mesh.

The surface chemical composition of the meshes was determined by EDS spectrum, and the results are shown in Fig. 2. The pure SSM contained Fe, Ni, and Cr, while the SSM-LDH also verified the presence of Al, Mg, Ca, Zn, and O elements. SSM-LDH/SA also contained C element in addition to the elements in SSM-LDH, originated from stearic acid in modified mesh.

It is important to note that such hierarchical structures do not alone contribute to the enhancement of superhydrophobicity or superoleophobicity of the mesh surfaces. Moreover, the surface energy (γ) is another important factor for producing superwetting surfaces (Ghasemi and Niakousari 2020). It can be expressed in terms of Gibbs free energy (G) by the following equation (Ghasemi and Niakousari 2020):

$$\gamma = \left(\frac{\partial G}{\partial A}\right)_{n,T,P} \tag{4}$$

where A is the surface area. The surface of molecules experiences excess energy due to intermolecular forces. Because of stronger intermolecular forces, the surface energy in hydrophilic surface including polar molecules is higher than that of hydrophobic surface containing nonpolar molecules.

In this regard, the high surface energy is critical for production of superoleophobic surfaces, which could be achieved by adding various hydrophilic functional groups. Also, the low surface energy is essential for preparation of superhydrophobic surfaces, which could be obtained by introducing hydrophobic agents such as stearic acid. Ascribed to synergetic effect of hierarchical rough structures and appropriate surface energy, the modified meshes demonstrated an improvement in superwetting properties.

Polarity and surface energy are directly related through the nature of intermolecular forces present at a material's surface (Israelachvili 2011). Polar surfaces possess molecules with permanent dipole moments, enabling strong interactions such as hydrogen bonding and dipole—dipole attractions. These strong cohesive forces result in high surface energy, making polar surfaces more likely to attract and interact with other polar substances, including water (i.e., they are hydrophilic). In contrast, nonpolar surfaces lack these dipole interactions, resulting in low surface energy. Such surfaces are typically hydrophobic and resist wetting by polar liquids. This relationship is often quantified using contact angle measurements, where polar surfaces yield low contact angles (good wettability) and nonpolar surfaces yield high contact angles (poor wettability).

The surface chemistry of the membranes was investigated by FT-IR spectroscopy to determine chemical composition of the membranes. As shown in Fig. 3, a wide



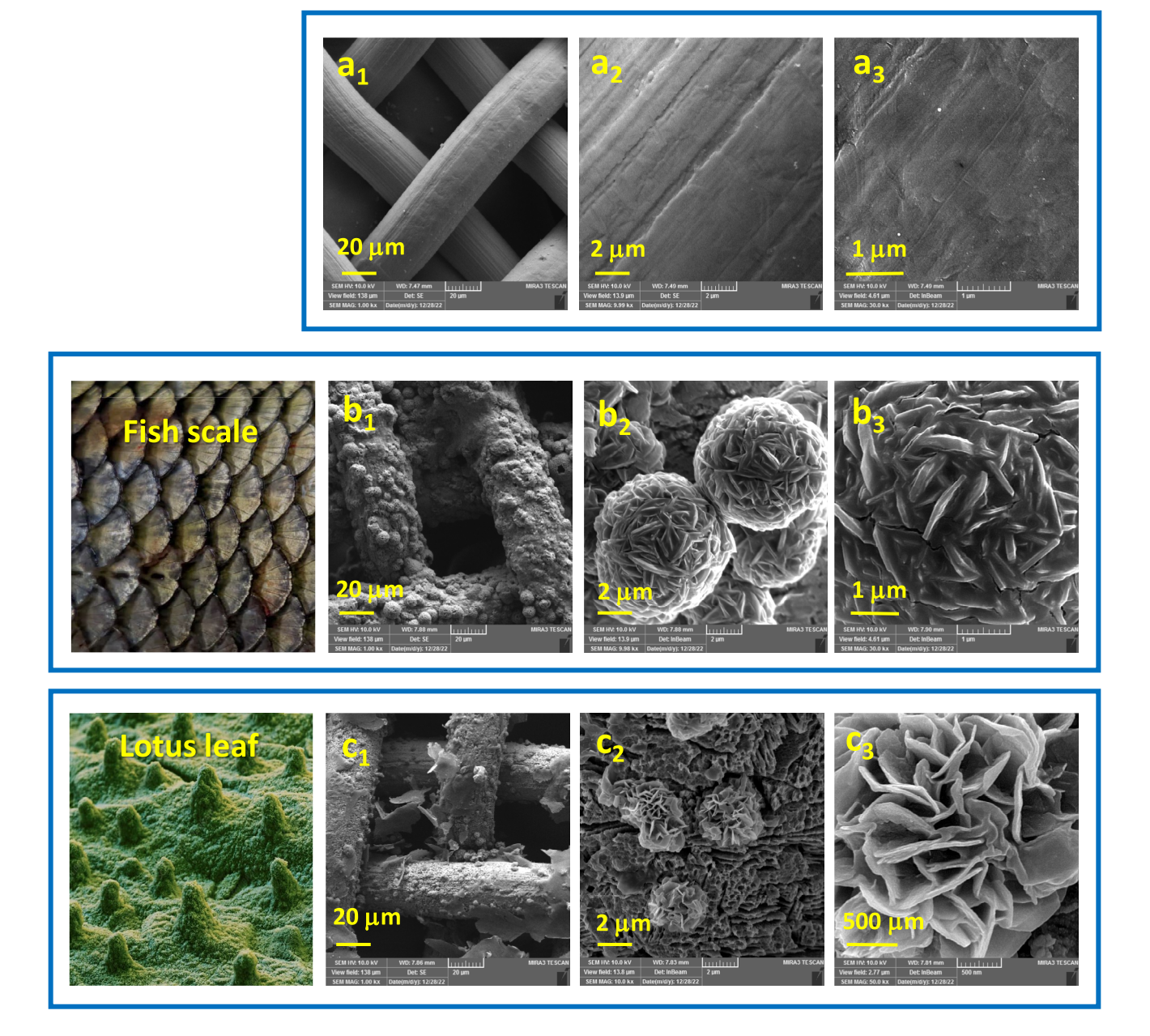


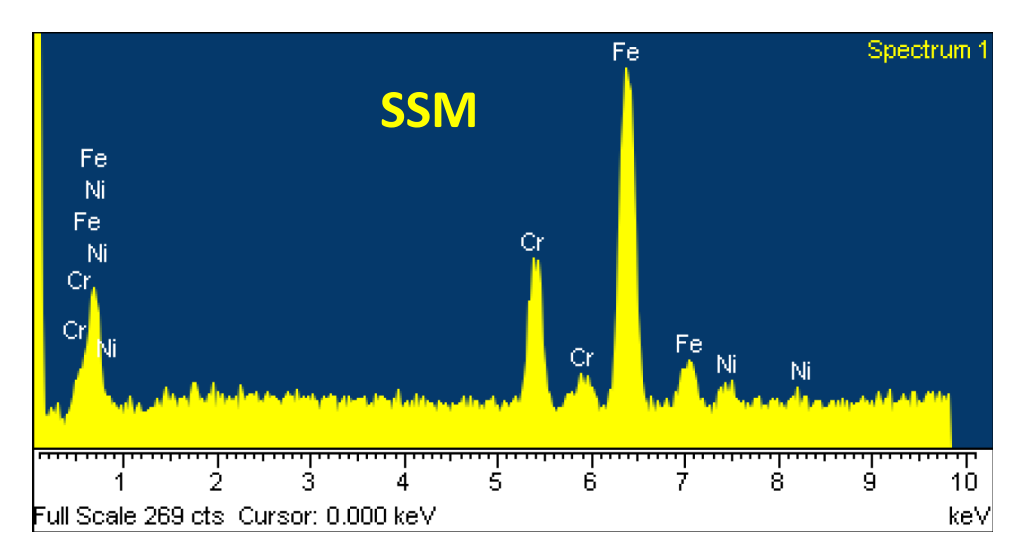
Fig. 1 FE-SEM images of (a_1-a_3) neat mesh; (b_1-b_3) fish-scale superhydrophilic-underwater superoleophobic SSM-LDH; (c_1-c_3) lotus leaf superhydrophobic-superoleophilic SSM-LDH/SA in different scales

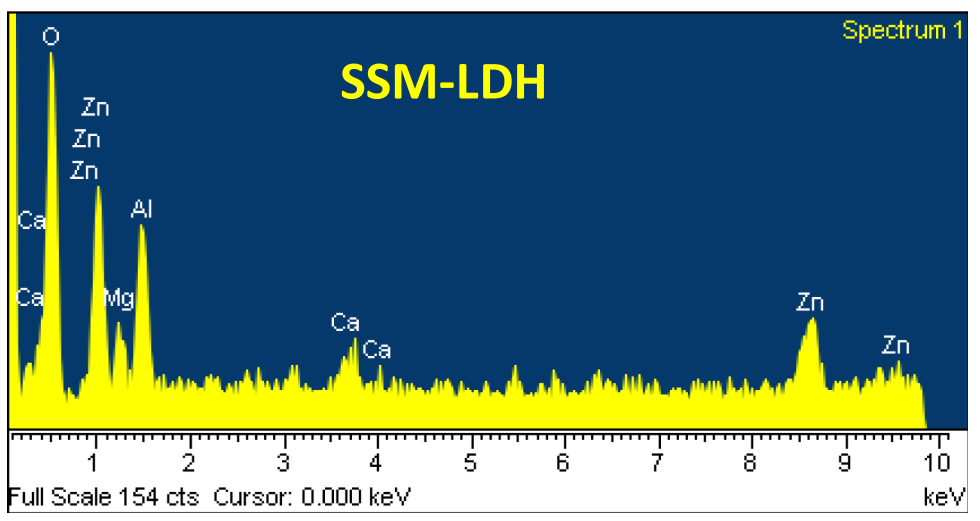
absorption peak at 3450 cm⁻¹ is attributed to the O–H stretching vibration. A narrow bond at 1638 cm⁻¹ is corresponded to the bending mode of the O–H resulted from water molecules in the interlayer spaces of LDHs. These O–H functional groups are responsible for superoleophobicity of the SSM-LDH. In addition, a band at 1384 cm⁻¹ comes from the presence of CO₃²⁻ anions in the interlayer region (Foroutan et al. 2023). According to the following reaction, urea is turned to ammonium and carbonate ions:

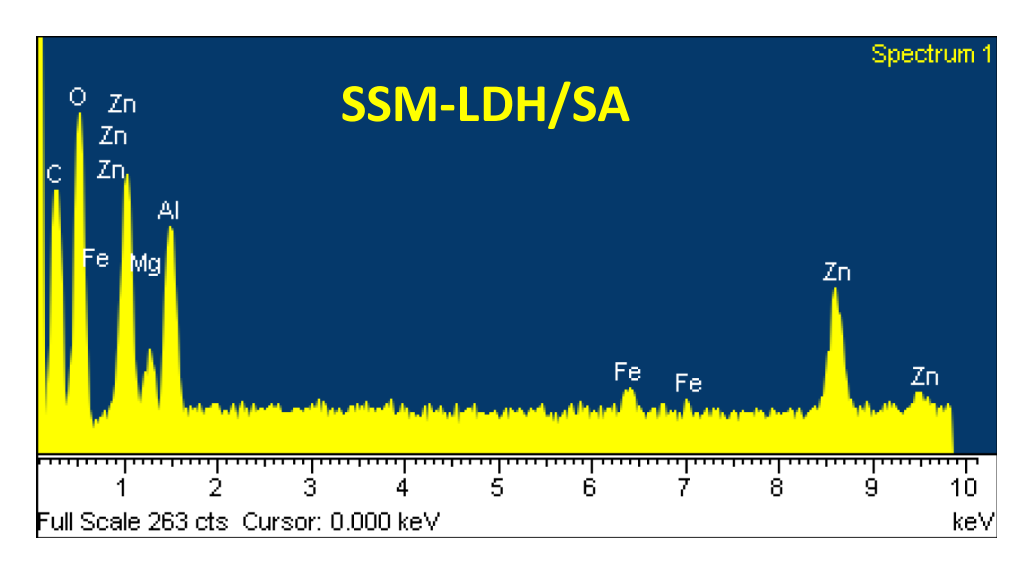
The characteristic bands at 450–800 cm⁻¹ are ascribed to metal–oxygen stretching vibration. It confirms that LDH has



Fig. 2 The EDS analysis of the neat mesh (SSM) and modified meshes (SSM-LDH and SSM-LDH/SA)







successfully coated on the surface of SSM. FT-IR spectra of SSM-LDH/SA shows two absorption bands at 2850 cm⁻¹ and 2920 cm⁻¹ which are attributed to the aliphatic C-H bonds in

SA. These aliphatic chains have led to superhydrophobicity of SSM-LDH/SA. Also, an absorption band at 1690 cm⁻¹ is related to stretching vibration of carboxylic groups.



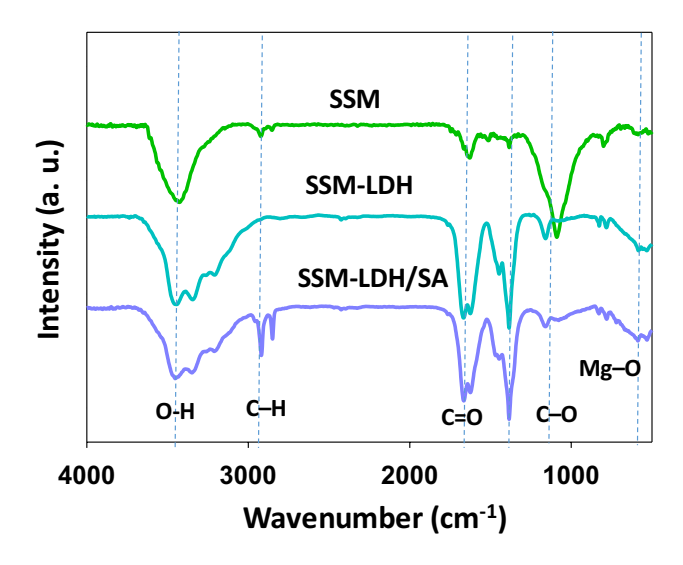


Fig. 3 FT-IR spectra of neat mesh (SSM); LDH coated mesh (SSM-LDH); and LDH/SA coated mesh (SSM-LDH/SA)

Surface wettability of the membranes

The surface wettability of the membranes was evaluated by dropping oil or water on the surface of meshes. As shown in Fig. 4a, a drop of water on the superhydrophobic surface of SSM-LDH/SA has maintained its spherical shape with WCA of $155 \pm 1.2^{\circ}$. Superhydrophobicity of SSM-LDH/SA was further verified by immersing a piece of mesh under water and formation of a silver mirror-like surface (Fig. 4b). This appearance is due to the mesh surface being surrounded by air bubbles, which prevents water from passing through membrane (Davardoostmanesh and Ahmadzadeh 2021). By changing the surface composition of the mesh to SSM-LDH, the surface wettability was inversed to superhydrophilic/ underwater superoleophobic. Figure 4c shows the spherical shape of a chloroform droplet on the surface of SSM-LDH confirming its underwater superoleophobicity. It is attributed to forming a water layer on the mesh surface that avoids the contact of oil with the mesh surface (Zhang et al. 2020b).

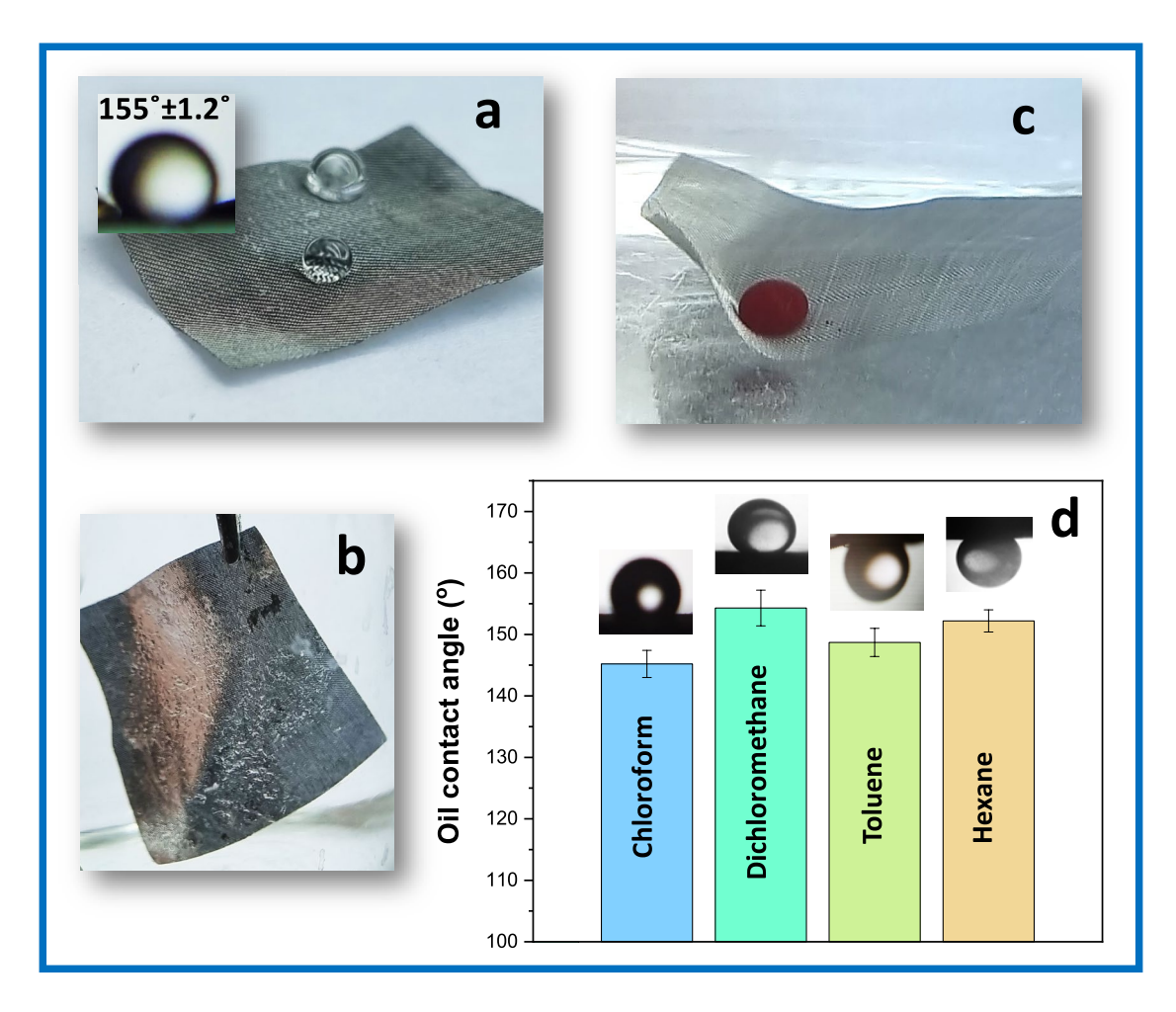


Fig. 4 (a) Image of a water droplet on the superhydrophobic SSM-LDH/SA with water contact angle of $155 \pm 1.2^{\circ}$; (b) the silver mirror-like image of SSM-LDH/SA under water; (c) image of a chloroform

droplet on the superhydrophilic SSM-LDH in water; (d) the underwater oil contact angles of SSM-LDH in some organic solvents



The OCAs of several types of organic solvents including chloroform, dichloromethane, toluene, and hexane were displayed in Fig. 4d. SSM-LDH shows the highest OCA of $153 \pm 1.9^{\circ}$ under water using dichloromethane, exhibiting the excellent superoleophobic performance.

Cassie-Baxter and Wenzel theories theoretically explain the role of surface roughness on the wetting properties of modified meshes (Onda 2022). For an ideal flat surface, Young's equation is applied in three phase system of liquid/ gas/solid (Jiang and Lin 2015):

$$\cos\theta_{lg} = \frac{\gamma_{sg} + \gamma_{sl}}{\gamma_{lg}} \tag{5}$$

where γ_{sg} , γ_{sl} , and γ_{lg} are the solid/gas, the solid/liquid, and the liquid/gas interface tensions, respectively. The Young's equation can also be applied to an oil/water/solid system as follows (Jiang and Lin 2015):

$$\cos\theta_{ow} = \frac{\gamma_{ws} + \gamma_{os}}{\gamma_{ow}} \tag{6}$$

where θ_{ow} is an OCA in water, γ_{ws} , γ_{os} , and γ_{ow} are the water/solid, the oil/solid, and the oil/water interface tensions, respectively. This equation can be extended as follows (Jiang and Lin 2015; Davardoostmanesh and Ahmadzadeh 2023a):

$$\cos\theta_{ow} = \frac{\gamma_{og}\cos\theta_o - \gamma_{wg}\cos\theta_w}{\gamma_{ow}} \tag{7}$$

where θ_o and θ_w are the oil and water CA in the air, respectively. γ_{og} and γ_{wg} are the interface tensions of the oil/gas and water/gas, respectively.

Generally, the surface tension of oils and organic solvents (γ_{og}) are in the range of 20–30 mN m⁻¹ and the water surface tension (γ_{wg}) is 73 mN m⁻¹ (Wang et al. 2018a). This means that increasing the hydrophilicity of the mesh decreases θ_w , which leads to an enhancement in underwater oleophobicity or θ_{ow} . Using Eq. 7, it can be found that an oleophilic surface in air becomes oleophobic under water. These interpretations can also be used for hydrophobic surfaces.

When it comes to rough surface, due to the formation of new interface on the micro-/nanostructures both oil and water CAs are increased (Jothi Prakash and Prasanth 2021). According to the Cassie-Baxter's model, in a hydrophobic surface, hierarchical structures can trap air forming a solid/gas interface in a liquid/gas/solid three-phase system (Sotoudeh et al. 2023). In an oleophobic surface, micro/nanostructures can trap water forming a liquid/solid interface in an oil/water/solid three-phase system. Therefore, the apparent water or oil CA ($\theta \prime$) in the air or water environment can be expressed by the following equation, respectively (Tang et al. 2023):

$$\cos\theta I = fI\cos\theta - (1 - fI) \tag{8}$$



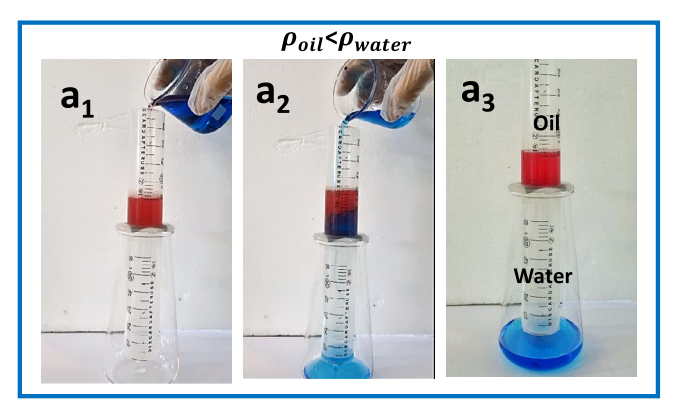
where f' is the area fraction of solid/liquid or oil/solid interfaces. For example, in a superhydrophobic surface, the water droplet is only in contact with the rough parts of the solid surface, leading to the large increase of water CA.

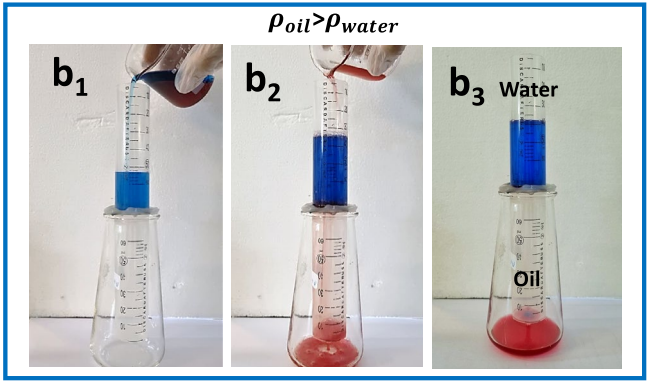
Oil-water separation performance

To investigate the separating ability of the prepared membranes, both light ($\rho_{oil} < \rho_{water}$) and heavy ($\rho_{oil} > \rho_{water}$) oil/ water mixtures were separated by SMM-LDH and SMM-LDH/SA, respectively. When using the SMM-LDH, only water can pass through membrane, while the oil is completely rejected. Thus, this type of membrane is more applicable for light oil/water mixture. For the light oil/water mixture, toluene/water mixture was used as an example as shown in Fig. 5a. Conversely, using SMM-LDH/SA, only oil penetrate through membrane and the water is blocked, completely. This type of membrane is appropriate for heavy oil/water mixture. Figure 5b shows the successful separation process of heavy oil/water mixture of chloroform/water through SMM-LDH/SA. The separation was conducted by passing the oil/water mixture with volume ratio of 1:2 through SSM-LDH and volume ratio of 2:1 through SSM-LDH/SA. The performance of the membranes is strongly influenced by the oil-to-water ratio. Superhydrophilic/underwater superoleophobic membranes (SSM-LDH) performed optimally when the water content is high, allowing water to permeate while effectively repelling oil, resulting in high separation efficiency and stable flux. However, as the oil content increases, excess oil accumulates on the membrane surface, leading to fouling and reduced efficiency. In contrast, superhydrophobic/superoleophilic membranes (SSM-LDH/SA) are most effective in oil-rich conditions, where oil readily permeates and water is repelled, ensuring high throughput and purity. When water dominates, these membranes suffer from water accumulation, reducing oil flux and potentially compromising the membrane's hydrophobic surface. Therefore, the separation efficiency and operational stability of both membrane types are closely tied to the oil/water ratio, emphasizing the importance of matching membrane wettability to feed composition or implementing bidirectional continuous system that can adapt to varying conditions.

The continuous system containing both meshes with inverse wettability can separate either light or heavy oil/water mixture (Fig. 5c). It is clear when the toluene or chloroform/water mixture was poured into the continuous system, both oil and water can quickly pass through membranes.

The separation efficiencies of each membrane with inverse wettability were calculated using Eq. 1 for several oil/water mixtures. The results in Fig. 6a shows that the separation efficiencies for all systems are in the ranges of





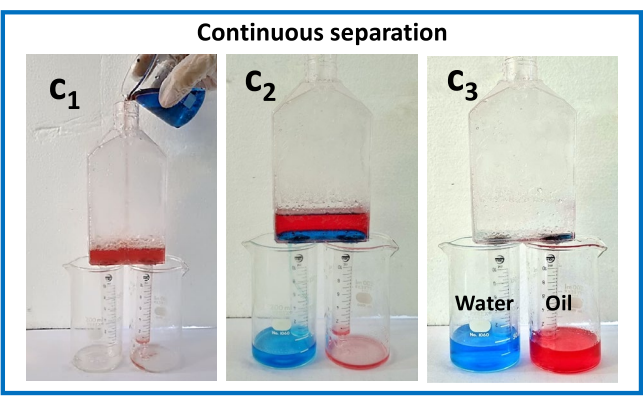


Fig. 5 The separation process of (a_1-a_3) toluene/water by SSM-LDH; (b_1-b_3) water/chloroform by SSM-LDH/SA; (c_1-c_3) toluene/water or water/chloroform by continuous system containing SSM-LDH and SSM-LDH/SA

98–99.7%. The separation efficiency depends on the physical and chemical properties of oil and organic solvents such as density, viscosity, polarity, and interfacial tension. It has an increase for low viscosity oils compared to high viscosity oils. More polar oils (e.g. those with functional groups such as esters, acids, or alcohols) interact more strongly with water, stabilizing emulsions. Nonpolar oils separate more readily due to weak interaction with water. In this regard, oils with high water solubility such as alcohols or aromatics are more difficult to separate. Higher interfacial tension between oil and water promotes easier phase separation under suitable condition. This means that oil and water are more strongly attracted to their own molecules than to each other.

Some of the physical and chemical characteristics of water and used organic solvents are shown in Table 1. There is a negligible difference between separation efficiencies because of the similar viscosity and density of various organic solvents. The results confirm that all kinds of oil/water mixtures could be efficiently separated by continuous system regardless of density differences.

To estimate the performance of modified meshes for fast oil/water separation, the permeation flux of oil and water through both membranes was individually measured (using Eq. 2), then, the liquid intrusion pressure was measured (using Eq. 3) to evaluate a stable selective separation. Finally, the results were compared with continuous system.

As cleared in Fig. 6b, SSM-LDH/SA with superhydrophobic properties, the maximum permeation flux of 12,200 Lm⁻²h⁻¹ was obtained in water/dichloromethane mixture. Also, SSM-LDH with superoleophobic properties shows the maximum water flux of 11,500 Lm⁻²h⁻¹ in toluene/water mixture.

One of the main problems of using one type of superwetting membrane in oil/water separation is accumulating one phase on top of the membrane surface during the separation process, which exerts increasing pressure on the mesh surface and limits the flow rate. Therefore, it is not possible to purify large amounts of oil/water mixture. The intrusion pressure indicates the capacity of a membrane to prevent liquid from passing through the membrane relative to another liquid (Kim et al. 2021). It can be calculated by measuring the maximum height of liquid that the mesh can withstand (using Eq. 3). The water intrusion pressure for superhydrophobic SSM-LDH/SA was measured 1.31 kPa. Also, the oil intrusion pressure of 1.13 kPa was obtained for underwater superoleophobic SSM-LDH using toluene solvent. These results confirm the stability of modified superwetting meshes during the separation of limited amounts of oil/water mixture (~20 mL). This means that



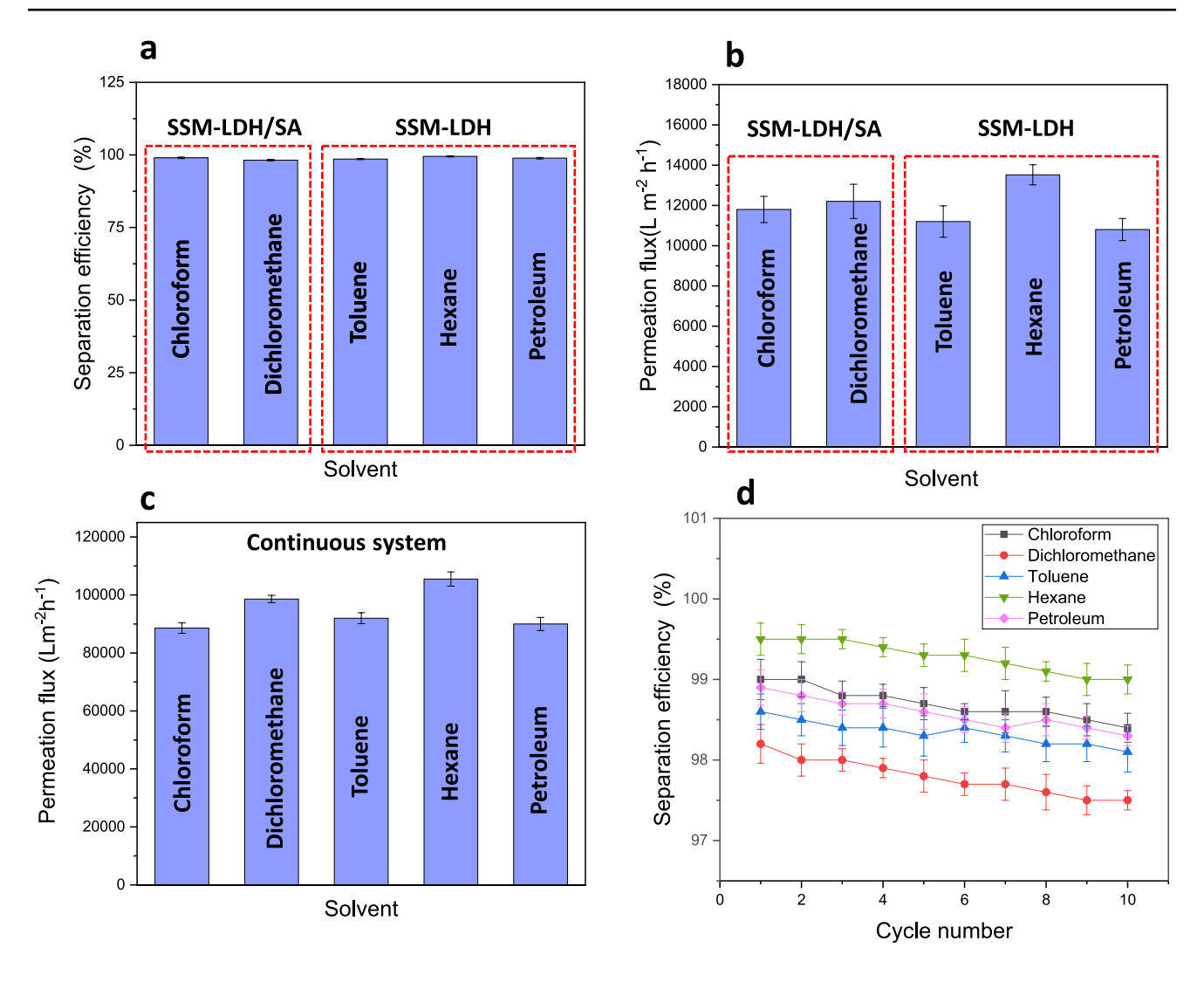


Fig. 6 FT-IR spectra Figure 6 (a) The separation efficiency for several types of heavy and light oils/water mixtures using SSM-LDH/SA and SSM-LDH, respectively; (b) permeation flux for several types of heavy and light oils/water mixtures using SSM-LDH/SA and SSM-LDH/SA and

LDH, respectively; (c) permeation flux for several types of heavy and light oil/water mixtures using continuous system containing both types of SSM-LDH/SA and SSM-LDH membranes on a system. (d) recyclability test for both SSM-LDH/SA and SSM/LDH membranes

Table 1 The physical and chemical characteristics of water and some organic solvents

Interfacial tension with water	Polarity	Water Solubility	Density (g/cm ³)	Viscosity (10 ⁻³ Pa s)	Solvent
-	Polar	-	0.998	0.89	Water
Low- moderate	Moderately polar	Moderate (~0.8 g/100 ml)	1.498	0.54	Chloroform
Low	Moderately polar	Moderate (~1.3 g/100 ml)	1.320	0.41	Dichloromethane
Moderate	Non-polar	Low (~0.05 g/100 ml)	0.867	0.55	Toluene
High	Non-polar	Very low (~0.001 g/100 ml)	0.655	0.29	n-hexane
High	Non-polar	Very low (<0.001 g/100 ml)	0.820-0.870	10–100	Petroleum



the purification of large amounts of oil/water mixture can cause mesh degradation. To solve this problem, two types of superwetting membrane with inverse wettability were simultaneously mounted on a system (Gong et al. 2020; Li et al. 2022). Doing so, oil and water were continuously passed through a superhydrophobic and a superhydrophilic mesh, respectively. Thus, accumulation of oils or water on top of the mesh and mesh destruction is prevented. Using this continuous separation system, large volumes of oil/water mixture could be purified at high flow rates. The permeation flux for passing 500 mL of different oil/water mixtures through continuous system is shown in Fig. 6c. The maximum permeation flux for toluene/water mixture was calculated 105,000 Lm⁻²h⁻¹.

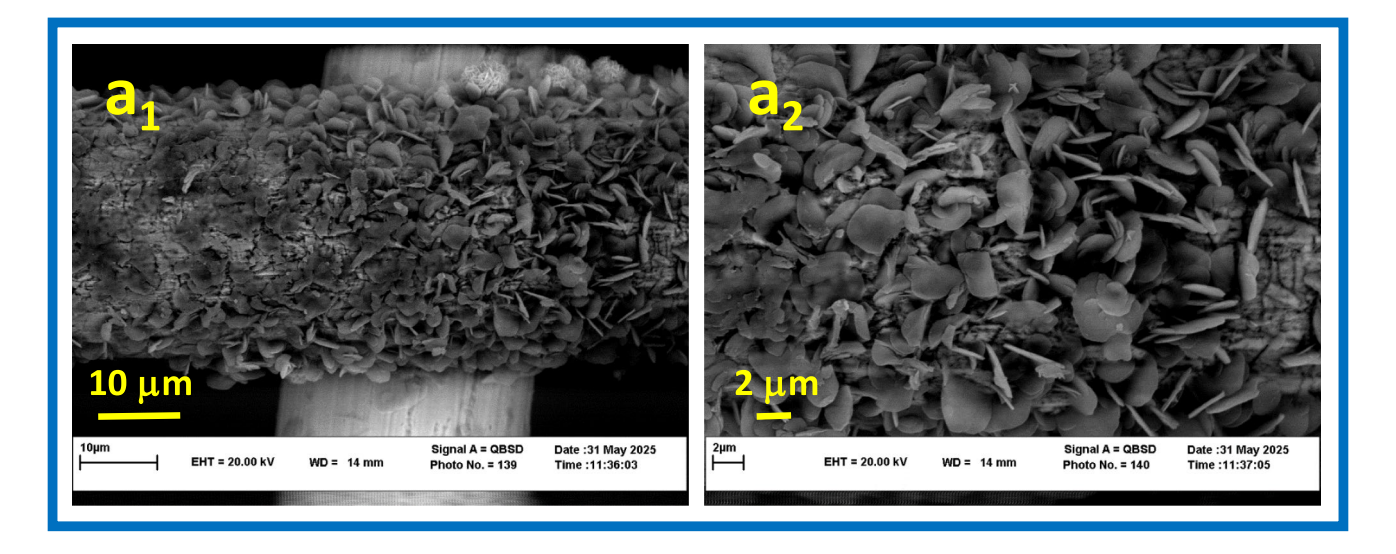
The recyclability of continuous system containing both SSM-LDH/SA and SSM-LDH was investigated by measuring the separation efficiencies of each superwetting meshes

for purification of a series of oil/water mixtures for 10 cycles. As shown in Fig. 6d, the separation efficiency shows negligible changes confirming good recyclability. The separation efficiencies were above 97.5% after 10 cycles.

Figure 7 shows the microstructural changes of the superwetting membranes after 10 cycles, confirming excellent stability of the membrane modifiers after several usages.

The influence of pH and temperature on the separation performance of the as-prepared meshes were determined. During practical application, coating materials may interact with corrosive and hot liquids. Therefore, the performance of the prepared membranes was evaluated under these conditions at different times. The separation efficiency of these membranes under harsh conditions is shown in Fig. 8.

The measurements of separation efficiencies of two types of membranes after immersion in alkaline and acidic solution indicate slightly decrease in separation efficiencies. It



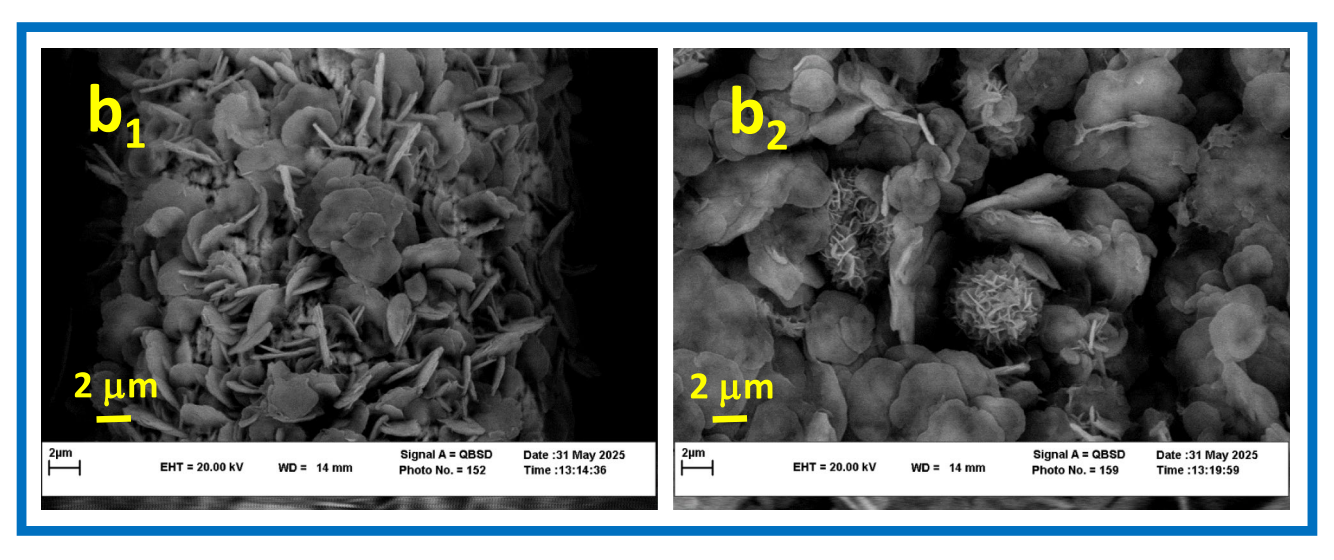


Fig. 7 SEM images of (a_1-a_2) SSM-LDH; and (b_1-b_3) SSM-LDH/SA after 10 cycles of oil-water separation

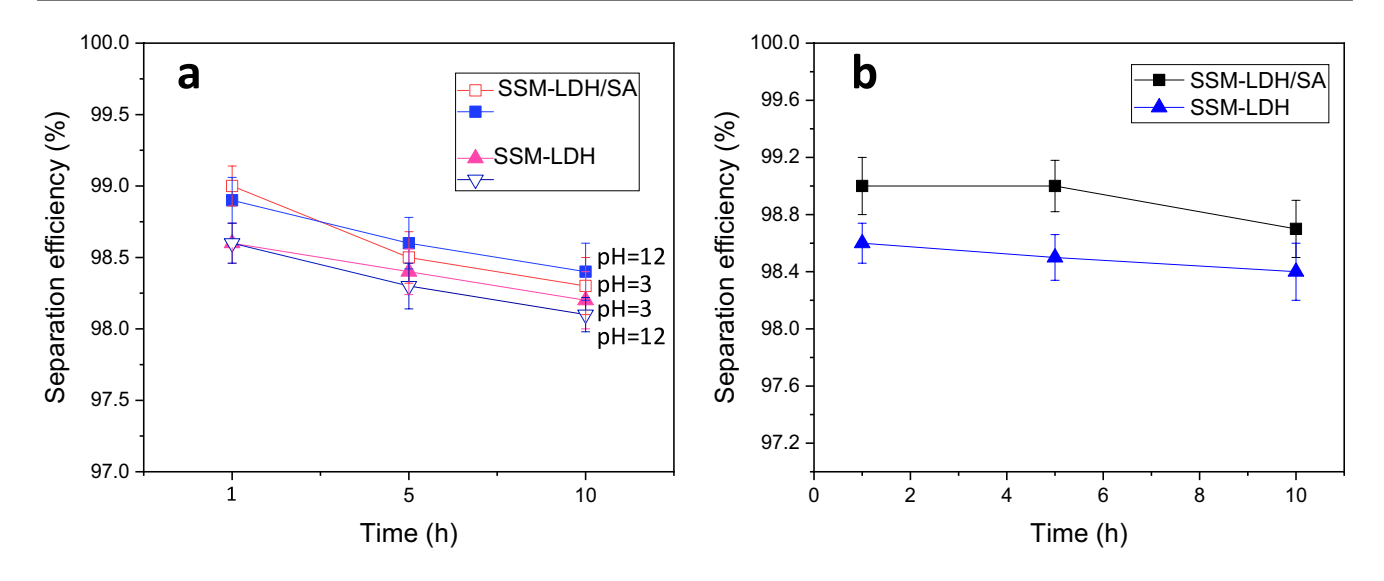


Fig. 8 The separation efficiency of SSM-LDH/SA and SSM-LDH at different times under harsh condition, respectively, (a) at different pH; (b) in hot water

could be due to dissolving LDH film in corrosive solutions. However, after immersion of the membranes in hot water (100 °C), their separation efficiencies remained unchanged for 5 h, signifying excellent thermal stability of the membranes.

Specifically, the antifouling behavior of the membranes is influenced by their surface wettability and micro/nano-structure. The superhydrophilic/underwater superoleophobic membrane (SSM-LDH) resists oil adhesion when submerged, preventing fouling by repelling oil droplets due to a stable hydration layer. Similarly, the superhydrophobic/superoleophilic membrane (SSM-LDH/SA) facilitates rapid oil transport while repelling water, which may contribute to membrane fouling after several cycles. It should be noted that the use of LDH contributes to fouling resistance due to its inherent chemical stability and hierarchical structure.

To evaluate the antifouling performance of the SSM-LDH/SA, the permeation flux for chloroform-water mixture

using SSM-LDH membrane was measured after 10 cycles. After each separation of the mixture, the membranes were washed with ethanol to be ready for the next experiment. After 10 cycles, the flux still kept a relatively high level of 10,000 Lm⁻²h⁻¹, indicating an outstanding antifouling performance of the SSM-LDH/SA, which is an important feature for the practical application.

Comparison performance

Unlike other studies that often rely on complex composites (e.g., PVA/montmorillonite, MOFs, or hydrogels) and multistep fabrication, this study achieves similar or superior performance using a more scalable and cost-effective approach. Some studies e.g., (Wang et al. 2018b) report comparable separation efficiencies, their systems are typically batch-operated and limited to either light or heavy oil separation. While comparable or slightly higher separation efficiencies (>99%) are

Table 2 Comparison performance of the bidirectional continuous LDH-based membrane with other studies

Material/System	Wettability Design	Efficiency	Flux (L·m ⁻² ·h ⁻¹)	Operation Mode	Ref
Bioinspired hierarchical surface	Superhydrophobic	~96%	~30,000	Batch	(Wang et al. 2018b)
PVA/montmorillonite composite on stainless steel mesh	Superhydrophilic/underwater superoleophobic	99.2%	37,098.6	Batch	(Dai et al. 2023)
Ni–Al LDH on cellulose membranes	Superhydrophobic/superoleo- philic	99.6%	1,412	Batch	(Wu et al. 2023)
Copper mesh with contrasting wettability	Integrated superhydrophilic and superhydrophobic system	>99%	Not specified	Continuous	(Huang et al. 2024)
LDH-coated stainless steel mesh	Dual-wettability (superhydro- philic/underwater superoleo- phobic and superhydrophobic/ superoleophilic)	>98%	105,000	Continuous, bidirectional	Current study



reported in literatures e.g., (Dai et al. 2023; Wu et al. 2023), these systems typically suffer from lower throughput and limited application scope (Table 2). Notably, the ultrahigh flux achieved in this study (105,000 Lm⁻²h⁻¹) far exceeds the values commonly reported (5,000–30,000 Lm⁻²h⁻¹), underscoring the design's potential for real-world application.

Conclusion

This study demonstrates the feasibility of continuous oil/ water separation by integrating two types of meshes with inverse wettability into a single system. Inspired by biological surfaces, a superhydrophilic mesh was fabricated by coating LDH onto a steel mesh, leveraging the intrinsic hydrophilicity of LDH. This mesh was then transformed into a superhydrophobic surface through the addition of SA, whose hydrophobic chains enhance water repellency. By combining these two meshes into a continuous system, gravity-driven separation of both light and heavy oil/water mixtures was achieved. The resulting dual-mesh system enables efficient separation of both light and heavy oil/water mixtures, regardless of their density differences. Both modified meshes exhibited separation efficiencies exceeding 98% across various oil/ water combinations. Notably, the permeation flux achieved in the continuous separation system was significantly higher than that of systems using a single type of superwetting mesh, with a maximum flux of 105,000 L m⁻²h⁻¹. This design overcomes a key limitation in conventional separation systems that often rely on a single type of wetting material and, therefore, cannot effectively handle mixtures with varying density relationships. Furthermore, the membranes maintained excellent recyclability over 10 separation cycles. This integrated and scalable system holds strong potential for rapid oil spill remediation and industrial water purification applications.

Acknowledgements The authors appreciate the support of the Ferdowsi University of Mashhad (61336).

Authors' contribution Maryam Davardoostmanesh: Conceptualization, Data curation, Formal analysis, Validation, Writing—original draft. Negin Gorgani: Data curation, Formal analysis, Investigation, Software, Funding acquisition, Hossein Ahmadzadeh: Conceptualization, Project administration, Validation, Visualization, Writing- review & editing.

Funding Ferdowsi University of Mashhad (61336).

Data availability All relevant data generated and analyzed during this study are included in this article. Other raw data files may be needed they are available from the corresponding author upon reasonable request.

Declarations

Ethical approval There are no ethical issues in this article.

Consent to participate All the authors agree to participate in this paper.

Consent for publication All the authors agree to the publication of this paper.

Competing interests The authors declare no competing interests.

References

- Chen Y, Quan Z, Song W, Wang Z, Li B, Mu Z, Niu S, Zhang J, Han Z, Ren L (2022) Hierarchically structured biomimetic membrane with mechanically/chemically durability and special wettability for highly efficient oil–water separation. Sep Purif Technol 300:121860. https://doi.org/10.1016/j.seppur.2022.121860
- Dai J, Wang L, Wang Y, Tian S, Tian X, Xie A, Zhang R, Yan Y, Pan J (2020) Robust nacrelike graphene oxide-calcium carbonate hybrid mesh with underwater superoleophobic property for highly efficient oil/water separation. ACS Appl Mater Interfaces 12:4482–4493. https://doi.org/10.1021/acsami.9b18664
- Dai X, Song Z, Li P, Li S, Yang L, Jiang Q (2023) Bioinspired superhydrophilic/underwater superoleophobic surfaces with robust wax-prevention, self-cleaning, and oil/water separation functions. New J Chem 47:2096–2106. https://doi.org/10.1039/D2NJ04991K
- Davardoostmanesh M, Ahmadzadeh H (2021) A mechanically flexible superhydrophobic rock wool modified with reduced graphene oxide-chloroperene rubber for oil-spill clean-up. Glob Challenges 5:2100072. https://doi.org/10.1002/gch2.202100072
- Davardoostmanesh M, Ahmadzadeh H (2023b) Remediation of saline oily water using an algae-based membrane. J Memb Sci 666:121201. https://doi.org/10.1016/J.MEMSCI.2022.121201
- Davardoostmanesh M, Ahmadzadeh H (2023a) Polyvinyl alcohol/ graphene oxide nanocomposite membrane for highly efficient oil/water mixture separation. Environ Prot Res 3:361–371. https://doi.org/10.37256/epr.3220233427
- Foroutan F, Ahmadzadeh H, Davardoostmanesh M, Amiri A (2023) Water desalination using stainless steel meshes coated with layered double hydroxide/graphene oxide nanocomposite. Water Environ Res 95:e10925. https://doi.org/10.1002/wer.10925
- Foroutan F, Davardoostmanesh M, Ahmadzadeh H (2025) Water desalination and methylene blue dye removal by microal-gae-based membrane: performance and mechanisms. Environ Sci Pollut Res 32:8084–8097. https://doi.org/10.1007/s11356-025-36166-0
- George G, Ealias AM, Saravanakumar MP (2024) Advancements in textile dye removal: a critical review of layered double hydroxides and clay minerals as efficient adsorbents. Environ Sci Pollut Res 31:12748–12779. https://doi.org/10.1007/s11356-024-32021-w
- Ghasemi A, Niakousari M (2020) Superwettability-based systems: basic concepts, recent trends and future prospects for innovation in food engineering. Trends Food Sci Technol 104:27–36. https://doi.org/10.1016/j.tifs.2020.07.027
- Gong Z, Yang N, Chen Z, Jiang B, Sun Y, Yang X, Zhang L (2020) Fabrication of meshes with inverse wettability based on the TiO2 nanowires for continuous oil/water separation. Chem Eng J 380:122524. https://doi.org/10.1016/j.cej.2019.122524
- Han L, Guo Y, Ning F, Liu X, Yi J, Luo Q, Qu B, Yue J, Lu Y, Li Q (2024) Lotus effect inspired hydrophobic strategy for stable zn metal anodes. Adv Mater 36:2308086. https://doi.org/10.1002/ adma.202308086
- Huang Z, Wang S, Shan X, Yin S, Tao B (2024) Superhydrophilic-superhydrophobic integrated system based on copper



- mesh for continuous and efficient oil-water separation. RSC Adv 14:6064-6071. https://doi.org/10.1039/D3RA08909F
- Israelachvili JN (2011) Intermolecular and surface forces. In: Intermolecular and surface forces. Elsevier, p 189
- Jiang L, Lin L (2015) Superoleophobicity of Fish Scales. Encyclopedia of Nanotechnology. Springer, Netherlands, Dordrecht, pp 1–7
- Jothi Prakash CG, Prasanth R (2021) Approaches to design a surface with tunable wettability: a review on surface properties J. Mater Sci 56:108–135. https://doi.org/10.1007/s10853-020-05116-1
- Kang H, Cheng Z, Lai H, Ma H, Liu Y, Mai X, Wang Y, Shao Q, Xiang L, Guo X, Guo Z (2018) Superlyophobic anti-corrosive and self-cleaning titania robust mesh membrane with enhanced oil/water separation. Sep Purif Technol 201:193–204. https://doi.org/10.1016/j.seppur.2018.03.002
- Kim D, Mauchauffé R, Kim J, Moon SY (2021) Simultaneous, efficient and continuous oil–water separation via antagonistically functionalized membranes prepared by atmospheric-pressure cold plasma. Sci Rep 11:3169. https://doi.org/10.1038/s41598-021-82761-9
- Li J, Long Y, Xu C, Tian H, Wu Y, Zha F (2018) Continuous, high-flux and efficient oil/water separation assisted by an integrated system with opposite wettability. Appl Surf Sci 433:374–380. https://doi.org/10.1016/j.apsusc.2017.10.056
- Li Y, He Y, Zhuang J, Shi H (2022) An intelligent natural fibrous membrane anchored with ZnO for switchable oil/water separation and water purification. Coll Surface A Physicochem Eng Asp 634:128041. https://doi.org/10.1016/j.colsurfa.2021.128041
- Liu P, Zhang Y, Liu S, Zhang Y, Qu L (2019) Fabrication of superhydrophobic marigold shape LDH films on stainless steel meshes via in-situ growth for enhanced anti-corrosion and high efficiency oil-water separation. Appl Clay Sci 182:105292. https://doi.org/ 10.1016/j.clay.2019.105292
- Liu R, Chen Q, Cao M, Lin J, Lin F, Ye W, Luis P, Van der Bruggen B, Zhao S (2021) Robust bio-inspired superhydrophilic and underwater superoleophobic membranes for simultaneously fast water and oil recovery. J Memb Sci 623:119041. https://doi.org/10.1016/j. memsci.2020.119041
- Onda T (2022) Theoretical investigation of Wenzel and Cassie wetting states on porous films and fiber meshes. Langmuir 38:13744–13752. https://doi.org/10.1021/acs.langmuir.2c01847
- Qing W, Li X, Wu Y, Shao S, Guo H, Yao Z, Chen Y, Zhang W, Tang CY (2020) In situ silica growth for superhydrophilicunderwater superoleophobic silica/PVA nanofibrous membrane for gravity-driven oil-in-water emulsion separation. J Memb Sci 612:118476. https://doi.org/10.1016/j.memsci.2020.118476
- Singh CJ, Mukhopadhyay S, Rengasamy RS (2022) Fibrous coalescence filtration in treating oily wastewater: a review. J Ind Text 51:3648S-3682S. https://doi.org/10.1177/15280837211040863
- Singh CJ, Mukhopadhyay S, Rengasamy RS, Srivastava M, Kumari R (2025a) Comparative analysis of Calotropis procera and Ceiba pentandra fibre-based filters used to separate oil from emulsified effluent. RSC Sustain 3:1751–1761. https://doi.org/10.1039/D5SU00068H
- Singh CJ, Srivastava M, Jaiswal V, Ghosh A, Mukhopadhyay S, Rengasamy RS (2025b) Cotton from industrial waste modified for effective absorption of oil spills. J Appl Polym Sci 142:e56773. https://doi.org/10.1002/app.56773
- Sotoudeh F, Mousavi SM, Karimi N, Lee BJ, Abolfazli-Esfahani J, Manshadi MKD (2023) Natural and synthetic superhydrophobic surfaces: A review of the fundamentals, structures, and applications. Alexandria Eng J 68:587–609. https://doi.org/10.1016/j.aej.2023.01.058
- Sow PK, Singhal R, Sahoo P, Radhakanth S (2021) Fabricating low-cost, robust superhydrophobic coatings with re-entrant topology for self-cleaning, corrosion inhibition, and oil-water separation. J Colloid Interface Sci 600:358–372. https://doi.org/10.1016/j.jcis.2021.05.026

- Tang S, Sun S, Liu T, Li M, Jiang Y, Wang D, Guo N, Guo Z, Chang X (2023) Bionic engineering-induced formation of hierarchical structured minerals with superwetting surfaces for oil-water separation. J Memb Sci 669:121261. https://doi.org/10.1016/j.memsci.2022.121261
- Wang L (2023) A critical review on robust self-cleaning properties of lotus leaf. Soft Matter 19:1058–1075. https://doi.org/10.1039/ D2SM01521H
- Wang H, Hu X, Ke Z, Du CZ, Zheng L, Wang C, Yuan Z (2018a) Review: Porous Metal Filters and Membranes for Oil-Water Separation. Nanoscale Res Lett 13:284. https://doi.org/10.1186/ s11671-018-2693-0
- Wang N, Wang Y, Shang B, Wen P, Peng B, Deng Z (2018b) Bioinspired one-step construction of hierarchical superhydrophobic surfaces for oil/water separation. J Colloid Interface Sci 531:300–310. https://doi.org/10.1016/j.jcis.2018.07.056
- Wu X, Feng S, Mao C, Liu C, Zhang Y, Zhou Y, Sheng X (2023) Superhydrophobic and superlipophilic LDH flower balls/cellulose membranes for efficient oil–water separation. New J Chem 47:7093–7100. https://doi.org/10.1039/D3NJ00847A
- Xiang Y, He Y, Zhang W, Li B, Li H, Wang Y, Yin X, Tang W, Li Z, He Z (2021) Superhydrophobic LDH/TTOS composite surface based on microstructure for the anti-corrosion, anti-fouling and oil-water separation application. Colloids Surfaces A Physicochem Eng Asp 622:126558. https://doi.org/10.1016/j.colsurfa.2021.126558
- Xie Y, Gu Y-H, Meng J, Yan X, Chen Y, Guo X-J, Lang W-Z (2020) Ultrafast separation of oil/water mixtures with layered double hydroxide coated stainless steel meshes (LDH-SSMs). J Hazard Mater 398:122862. https://doi.org/10.1016/j.jhazmat.2020.122862
- Xin Y, Qi B, Wu X, Yang C, Li B (2024) Different types of membrane materials for oil-water separation: Status and challenges. Colloid Interface Sci Commun 59:100772. https://doi.org/10.1016/j.colcom.2024.100772
- Xu S, Wang Q, Wang N (2021) Chemical fabrication strategies for achieving bioinspired superhydrophobic surfaces with micro and nanostructures: a review. Adv Eng Mater 23:2001083. https://doi. org/10.1002/adem.202001083
- Zhang J, Fang W, Zhang F, Gao S, Guo Y, Li J, Zhu Y, Zhang Y, Jin J (2020a) Ultrathin microporous membrane with high oil intrusion pressure for effective oil/water separation. J Memb Sci 608:118201. https://doi.org/10.1016/j.memsci.2020.118201
- Zhang Y, Wang H, Liu B, Zhao X, Wei Y (2020b) NiCo2O4 hierarchical structure coated mesh with long-term stable underwater superoleophobicity for high-efficient, high-flux oil-water separation. Appl Surf Sci 504:144598. https://doi.org/10.1016/j.apsusc. 2019.144598
- Zhao W, Wang Y, Han M, Xu J, Tam KC (2022) Surface Modification, Topographic Design and Applications of Superhydrophobic Systems. Chem – A Eur J 28:e202202657. https://doi.org/10.1002/ chem.202202657
- Zhou D-L, Yang D, Han D, Zhang Q, Chen F, Fu Q (2021) Fabrication of superhydrophilic and underwater superoleophobic membranes for fast and effective oil/water separation with excellent durability. J Memb Sci 620:118898. https://doi.org/10.1016/j.memsci. 2020.118898

Publisher's Note Springer Nature remains neutral with regard to jurisdictional claims in published maps and institutional affiliations.

Springer Nature or its licensor (e.g. a society or other partner) holds exclusive rights to this article under a publishing agreement with the author(s) or other rightsholder(s); author self-archiving of the accepted manuscript version of this article is solely governed by the terms of such publishing agreement and applicable law.

